

We are IntechOpen, the world's leading publisher of Open Access books Built by scientists, for scientists

6,900

Open access books available

186,000

International authors and editors

200M

Downloads

Our authors are among the

154

Countries delivered to

TOP 1%

most cited scientists

12.2%

Contributors from top 500 universities



WEB OF SCIENCE™

Selection of our books indexed in the Book Citation Index
in Web of Science™ Core Collection (BKCI)

Interested in publishing with us?
Contact book.department@intechopen.com

Numbers displayed above are based on latest data collected.
For more information visit www.intechopen.com



Bioheat Transfer

Alireza Zolfaghari¹ and Mehdi Maerefat²

¹*Department of Mechanical Engineering, Birjand University, Birjand,*

²*Department of Mechanical Engineering, Tarbiat Modares University, Tehran, Iran*

1. Introduction

Heat transfer in living tissues is a complicated process because it involves a combination of thermal conduction in tissues, convection and perfusion of blood, and metabolic heat production. Over the years, several mathematical models have been developed to describe heat transfer within living biological tissues. These models have been widely used in the analysis of hyperthermia in cancer treatment, laser surgery, cryosurgery, cryopreservation, thermal comfort, and many other applications. The most widely used bioheat model was introduced by Pennes in 1948. Pennes proposed a new simplified bioheat model to describe the effect of blood perfusion and metabolic heat generation on heat transfer within a living tissue. Since the landmark paper by Pennes (1948), his model has been widely used by many researchers for the analysis of bioheat transfer phenomena. And, also a large number of bioheat transfer models have been proposed to overcome the shortcomings of Pennes' equation. These models include the continuum models which consider the thermal impact of all blood vessels as a global parameter and the vascular models which consider the thermal impact of each vessel individually.

Although, several bioheat models have been developed in the recent years, the thermoregulatory control mechanisms of the human body such as shivering, regulatory sweating, vasodilation, and vasoconstriction have not been considered in these models. On the other hand, these mechanisms may significantly influence the thermal conditions of the human body. This causes a serious limitation in using the bioheat models for evaluating the human body thermal response. In order to remove this limitation, Zolfaghari and Maerefat (2010) developed a new Simplified Thermoregulatory Bioheat (STB) model based on the combination of the well-known Pennes' equation and Gagge's thermal comfort model.

The present chapter aims at giving a concise introduction to bioheat transfer and the mathematical models for evaluating the heat transfer within biological tissues. This chapter is divided into six sections. The first section presents an introduction to the concept and history of bioheat transfer. The structure of living tissues with blood perfusion is described in section 2. Next, third section focuses on the mathematical modelling of heat transfer in living tissues. In the mentioned section, a brief description of some of the most important bioheat models (i.e. Pennes (1948) model, Wulff (1974) model, Klinger (1974) model, Chen and Holmes (1980) model and so on) is presented. Afterwards, section 4 explains the complexity of evaluating heat transfer within the tissues that thermally controlled by thermoregulatory mechanisms such as shivering, regulatory sweating, vasodilation, and

vasoconstriction. Then, the Simplified Thermoregulatory Bioheat (STB) model is introduced for evaluating heat transfer within the segments of the human body. Finally, section 5 outlines the main conclusions and recommendations of the research. Moreover, the selected references are listed in the last section.

2. Structure of blood perfused tissues

Before we discuss the bioheat models, let us have a brief look at the structure of blood perfused tissues. The biological tissues include the layers of skin, fat, muscle and bone. Moreover, the skin is composed of two stratified layers: epidermis and dermis. Fig. 1 shows a schematic geometry of the tissue structure. Furthermore, the thermophysical properties of the human body tissue are provided in Table 1 (Lv & Liu, 2007; Sharma, 2010).

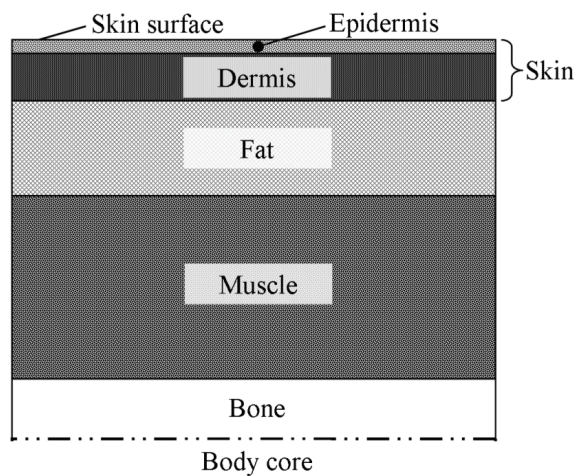


Fig. 1. Schematic geometry of the tissue structure (figure not to scale)

	Thickness	Density	Specific heat	Blood perfusion rate	Thermal conductivity
	l (m)	ρ (kg/m ³)	C (J/kg K)	W_{bl} (m ³ /s m ³)	k (W/m K)
Epidermis	80×10^{-6}	1200	3589	0	0.24
Dermis	0.002	1200	3300	0.00125	0.45
Fat	≈ 0.010	937	3258	0.00125	0.21
Muscle	≈ 0.020	1000	4000	0.00125	0.5
Bone	≈ 0.008	1920	1440	-	0.44
Blood	-	937	3889	-	0.64

Table 1. Geometrical information and thermal properties of the human body tissue (Lv & Liu, 2007; Sharma, 2010)

Blood circulation is a key mechanism for regulating the body temperature. The circulatory system of the human body comprises of two sets of blood vessels (arteries and veins) which carry blood from the heart and back. Blood leaves the heart through the aorta, which is the largest artery (diameter $\approx 5000\text{ }\mu\text{m}$). Vessels supplying blood to muscles are known as main supply arteries and veins (SAV, 300-1000 μm diameter). They branch into primary arteries, (P, 100-300 μm diameter) which feed the secondary arteries (s, 50-100 μm diameter). These

vessels deliver blood to the arterioles (20-40 μm diameter) which supply blood to the smallest vessels known as capillaries (c, 5-15 μm diameter). Blood is returned to the heart through a system of vessels known as veins. Fig. 2 shows a schematic diagram of a typical vascular structure (Jiji, 2009).

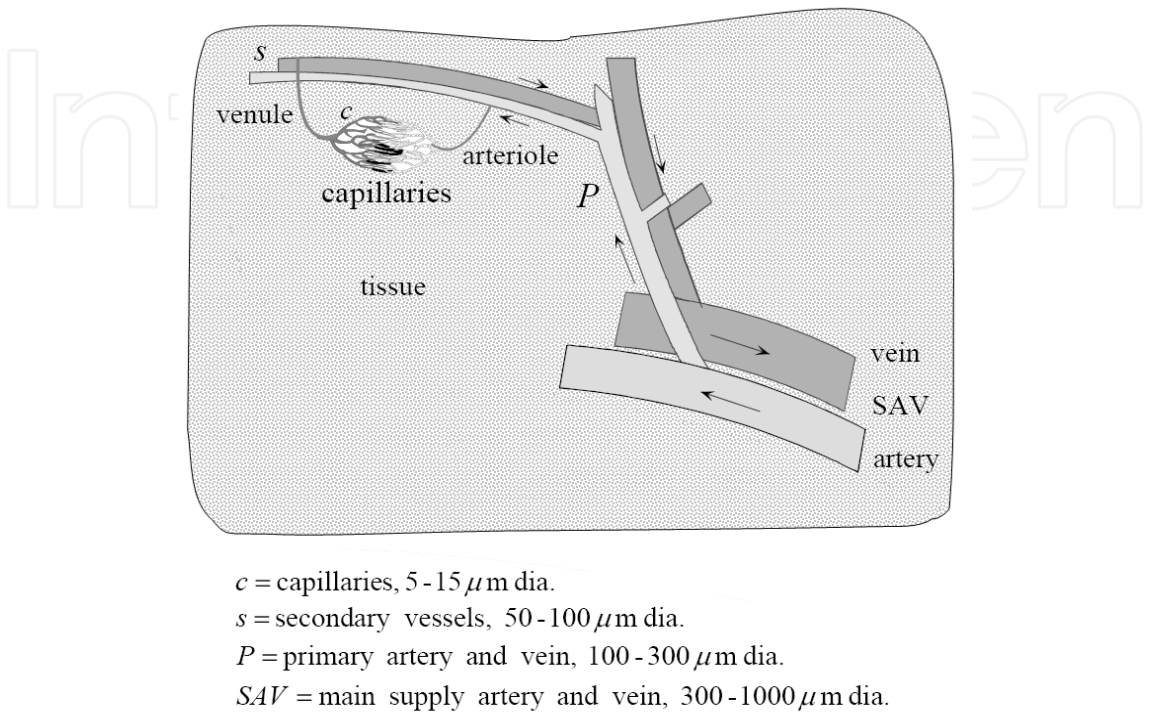


Fig. 2. Schematic diagram of the vascular system (Jiji, 2009)

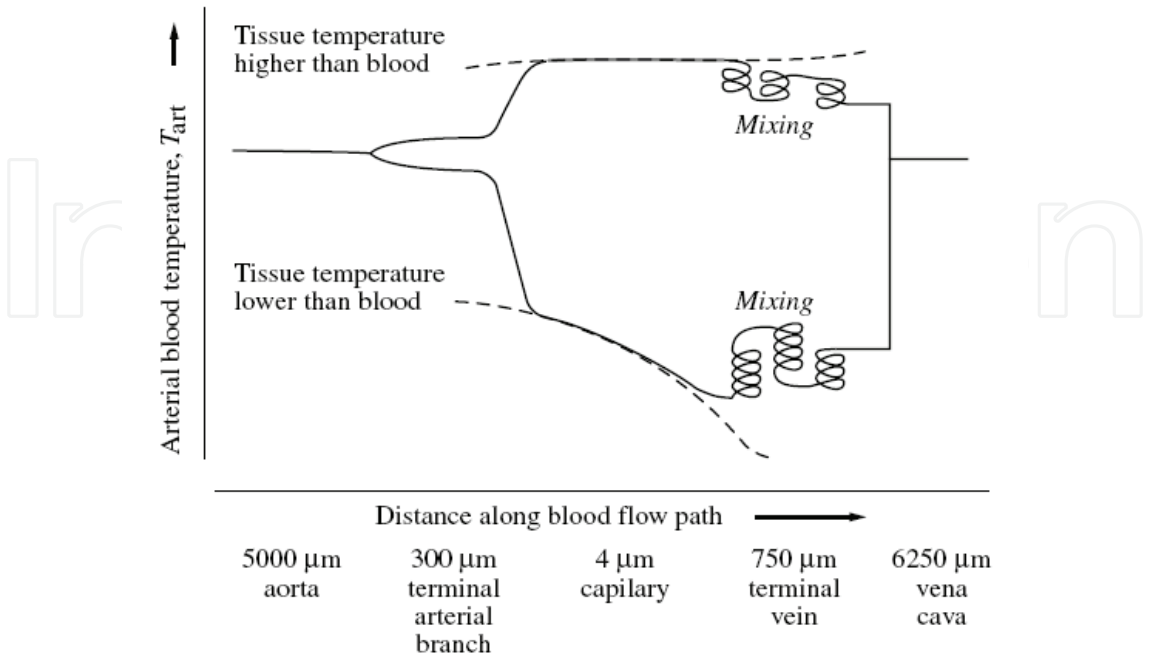


Fig. 3. Schematic of temperature equilibration between the blood and the tissue (Datta, 2002)

Blood leaves the heart at the arterial temperature T_{art} . It remains essentially at this temperature until it reaches the main arteries where equilibration with surrounding tissue begins to take place. Equilibration becomes complete prior to reaching the arterioles and capillaries. Beyond this point, blood temperature follows the solid tissue temperature (T_{ti}) through its spatial and time variations until blood reaches the terminal veins. At this point the blood temperature ceases to equilibrate with the tissue, and remains virtually constant, except as it mixes with other blood of different temperatures at venous confluences. Finally, the cooler blood from peripheral regions and warmer blood from internal organs mix within the vena cava and the right atrium and ventricle. Following thermal exchange in the pulmonary circulation and remixing in the left heart, the blood attains the same temperature it had at the start of the circuit (Datta, 2002). Fig. 3 shows a schematic of temperature equilibration between the blood and the solid tissue.

3. Mathematical models of bioheat transfer

3.1 Pennes model

Over the years, the effects of blood flow on heat transfer in living tissue have been studied by many researchers and a large number of bioheat transfer models have been developed on the basis of two main approaches: the continuum approach and the discrete vessel (vascular) approach. In the continuum approach, the thermal impact of all blood vessels models with a single global parameter; and the vascular approach models the impact of each vessel individually (Raaymakers et al., 2009). The most widely used continuum model of perfused tissue was introduced in 1948 by Harry Pennes. The Pennes (1948) model was initially developed for predicting heat transfer in the human forearm. Due to the simplicity of the Pennes bioheat model, it was implemented in various biological research works such as for therapeutic hyperthermia for the treatment of cancer (Minkowycz et al., 2009).

Pennes bioheat model is based on four simplifying assumptions (Jiji, 2009):

1. All pre-arteriole and post-venule heat transfer between blood and tissue is neglected.
2. The flow of blood in the small capillaries is assumed to be isotropic. This neglects the effect of blood flow directionality.
3. Larger blood vessels in the vicinity of capillary beds play no role in the energy exchange between tissue and capillary blood. Thus the Pennes model does not consider the local vascular geometry.
4. Blood is assumed to reach the arterioles supplying the capillary beds at the body core temperature. It instantaneously exchanges energy and equilibrates with the local tissue temperature.

Based on these assumptions, Pennes (1948) modeled blood effect as an isotropic heat source or sink which is proportional to blood flow rate and the difference between the body core temperature and local tissue temperature. Therefore, Pennes (1948) proposed a model to describe the effects of metabolism and blood perfusion on the energy balance within tissue. These two effects were incorporated into the standard thermal diffusion equation, which is written in its simplified form as:

$$\rho_{ti} C_{ti} \frac{\partial T_{ti}}{\partial t} = \nabla \cdot k_{ti} \nabla T_{ti} + \rho_{bl} C_{bl} W_{bl} (T_{art} - T_{ti}) + q_m \quad (1)$$

where ρ_{ti} , C_{ti} , T_{ti} and k_{ti} are, respectively, the density, specific heat, temperature and thermal conductivity of tissue. Also, T_{art} is the temperature of arterial blood, q_m is the metabolic heat

generation and ρ_{bl} , C_{bl} and W_{bl} are, respectively, the density, specific heat and perfusion rate of blood. It should be noted that metabolic heat generation is assumed to be homogeneously distributed throughout the tissue. Also, it is assumed that the blood perfusion effect is homogeneous and isotropic and that thermal equilibration occurs in the microcirculatory capillary bed. In this scenario, blood enters capillaries at the temperature of arterial blood, T_{art} , where heat exchange occurs to bring the temperature to that of the surrounding tissue, T_{ti} . There is assumed to be no energy transfer either before or after the blood passes through the capillaries, so that the temperature at which it enters the venous circulation is that of the local tissue (Kreith, 2000).

Pennes (1948) performed a series of experimental studies to validate his model. Validations have shown that the results of Pennes bioheat model are in a reasonable agreement with the experimental data. Although Pennes bioheat model is often adequate for roughly describing the effect of blood flow on the tissue temperature, there exist some serious shortcomings in his model due to its inherent simplicity. The shortcomings of Pennes bioheat model come from the basic assumptions that are introduced in this model. These shortcomings can be listed as follows (Jiji, 2009):

1. Thermal equilibration does not occur in the capillaries, as Pennes assumed. Instead it takes place in pre-arteriole and post-venule vessels having diameters ranging from 70-500 μm .
2. Directionality of blood perfusion is an important factor in the interchange of energy between vessels and tissue. The Pennes equation does not account for this effect.
3. Pennes equation does not consider the local vascular geometry. Thus significant features of the circulatory system are not accounted for. This includes energy exchange with large vessels, countercurrent heat transfer between artery-vein pairs and vessel branching and diminution.
4. The arterial temperature varies continuously from the deep body temperature of the aorta to the secondary arteries supplying the arterioles, and similarly for the venous return. Thus, contrary to Pennes' assumption, pre-arteriole blood temperature is not equal to body core temperature and vein return temperature is not equal to the local tissue temperature. Both approximations overestimate the effect of blood perfusion on local tissue temperature.

To overcome these shortcomings, a considerable number of modifications have been proposed by various researchers. Wulff (1974) and Klinger (1974) considered the local blood mass flux to account the blood flow direction, while Chen and Holmes (1980) examined the effect of thermal equilibration length on the blood temperature and added the dispersion and microcirculatory perfusion terms to the Klinger equation (Vafai, 2011). In the following sections, a brief review of the modified bioheat models will be given.

3.2 Wulff continuum model

Due to the simplicity of the Pennes model, many authors have looked into the validity of the assumptions used to develop the Pennes bioheat equation. Wulff (1974) was one of the first researchers that directly criticized the fundamental assumptions of the Pennes bioheat equation and provided an alternate analysis (Cho, 1992). Wulff (1974) assumed that the heat transfer between flowing blood and tissue should be modeled to be proportional to the temperature difference between these two media rather than between the two bloodstream temperatures (i.e., the temperature of the blood entering and leaving the tissue). Thus, the energy flux at any point in the tissue should be expressed by (Minkowycz et al., 2009)

$$q = -k_{ti} \nabla T_{ti} + \rho_{bl} h_{bl} v_h \quad (2)$$

where v_h is the local mean blood velocity. Moreover, h_{bl} is the specific enthalpy of the blood and it is given by

$$h_{bl} = \int_{T_o}^{T_{bl}} C_{bl}(T_{bl}^*) dT_{bl}^* + \frac{P}{\rho_{bl}} + \Delta H_f (1 - \phi) \quad (3)$$

where P is the system pressure, ΔH_f is the enthalpy of formation of the metabolic reaction, and ϕ is the extent of reaction. Also, T_o and T_{bl} are the reference and blood temperatures, respectively. Thus, the energy balance equation can be written as

$$\rho_{ti} C_{ti} \frac{\partial T_{ti}}{\partial t} = -\nabla \cdot q \quad (4)$$

Therefore,

$$\rho_{ti} C_{ti} \frac{\partial T_{ti}}{\partial t} = -\nabla \cdot \left[-k_{ti} \nabla T_{ti} + \rho_{bl} v_h \left(\int_{T_o}^{T_{bl}} C_{bl}(T_{bl}^*) dT_{bl}^* + \frac{P}{\rho_{bl}} + \Delta H_f (1 - \phi) \right) \right] \quad (5)$$

Neglecting the mechanical work term (P/ρ_{bl}), setting the divergence of $\rho_{bl} v_h$ to zero, and assuming constant physical properties, Eq. (5) can be simplified as follows (Minkowycz et al., 2009):

$$\rho_{ti} C_{ti} \frac{\partial T_{ti}}{\partial t} = k_{ti} \nabla^2 T_{ti} - \rho_{bl} C_{bl} v_h \nabla T_{bl} + \rho_{bl} v_h \Delta H_f \nabla \phi \quad (6)$$

Since blood is effectively microcirculating within the tissue, it will likely be in thermal equilibrium with the surrounding tissue. As such, Wulff (1974) assumed that T_{bl} is equivalent to the tissue temperature T_{ti} . In this condition, the metabolic reaction term ($\rho_{bl} v_h \Delta H_f \nabla \phi$) is equivalent to q_m . Therefore, the final form of the bioheat equation that was derived by Wulff (1974) is

$$\rho_{ti} C_{ti} \frac{\partial T}{\partial t} = k_{ti} \nabla^2 T_{ti} - \rho_{bl} C_{bl} v_h \cdot \nabla T_{ti} + q_m \quad (7)$$

It should be noted that the main challenge in solving this bioheat equation is in the evaluation of the local blood mass flux $\rho_{bl} v_h$ (Minkowycz et al., 2009).

3.3 Klinger continuum model

In 1974, Klinger presented an analytical bioheat model that was conceptually similar to Wulff bioheat model. Klinger (1974) argued that in utilizing the Pennes model, the effects of nonunidirectional blood flow were being neglected and thus significant errors were being introduced into the computed results. In order to correct this lack of directionality in the formulation, Klinger (1974) proposed that the convection field inside the tissue should be modeled based upon the *in vivo* vascular anatomy (Cho, 1992). Taking into account the spatial and temporal variations of the velocity and heat source, and assuming constant physical properties of tissue and incompressible blood flow, the Klinger bioheat equation was expressed as:

$$\rho_{ti}C_{ti}\frac{\partial T}{\partial t}=k_{ti}\nabla^2T_{ti}-\rho_{bl}C_{bl}\mathbf{v}\cdot\nabla T_{ti}+q_m \quad (8)$$

This equation is similar to that derived by Wulff (1974), except it is written for the more general case of a spatially and temporally nonuniform velocity field (\mathbf{v}) and heat source (q_m).

3.4 Chen-Holmes (CH) continuum model

Among the continuum bioheat models, the Chen-Holmes model (Chen & Holmes, 1980) is the most developed (Kreith, 2000). Chen and Holmes (1980) showed that the major heat transfer processes occur in the 50 to 500 μm diameter vessels. Consequently, they proposed that larger vessels be modeled separately from smaller vessels and tissue. Therefore, in the Chen-Holmes bioheat model, the total tissue control volume is subdivided to the solid-tissue subvolume (V_s) and blood subvolume (V_b) as shown in Fig. 4. By using this concept, Chen and Holmes (1980) proposed a new modified relationship for calculating the blood perfusion term (q_{bl}) in their bioheat model:

$$q_{bl}=\rho_{bl}C_{bl}W_{bl}^*(T_{art}^*-T_{ti})-\rho_{bl}C_{bl}\mathbf{v}\cdot\nabla T_{ti}+\nabla.k_p\nabla T_{ti} \quad (9)$$

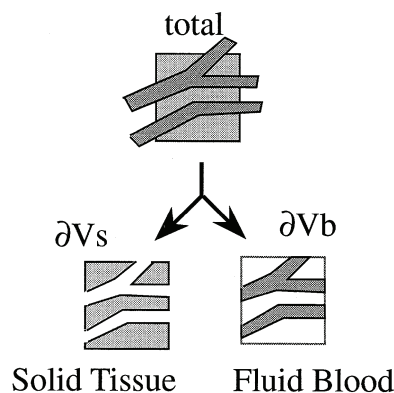


Fig. 4. Schematic representation of tissue control volume as used in Chen-Holmes model (Kreith, 2000)

In Eq. (9), the first term on the right hand side appears similar to Pennes' perfusion term except the perfusion rate (W_{bl}^*) and the arterial temperature (T_{art}^*) are specific to the volume being considered. It should be noted that T_{art}^* is essentially the temperature of blood upstream of the arterioles and it is not equal to the body core temperature. The second term in Eq. (9) accounts for energy convected due to equilibrated blood. Directionality of blood flow is described by the vector \mathbf{v} , which is the volumetric flow rate per unit area. The third term in Eq. (9) describes conduction mechanisms associated with small temperature fluctuations in equilibrated blood. The symbol k_p denotes "perfusion conductivity". It is a function of blood flow velocity, vessel inclination angle relative to local temperature gradient, vessel radius and number density.

Using a simplified volume-averaging technique, the Chen-Holmes bioheat equation can be written as follows:

$$\rho_{ti,eff}C_{ti,eff}\frac{\partial T_{ti}}{\partial t}=\nabla.k_{ti,eff}\nabla T_{ti}-\left\{\rho_{bl}C_{bl}W_{bl}^*(T_{art}^*-T_{ti})-\rho_{bl}C_{bl}\mathbf{v}\cdot\nabla T_{ti}+\nabla.k_p\nabla T_{ti}\right\}+q_m \quad (10)$$

where

$$\rho_{ti,eff} = (1 - \varepsilon_{bl})\rho_{ti} + \varepsilon_{bl}\rho_{bl} \quad (11)$$

$$C_{ti,eff} = (1 - \varepsilon_{bl})C_{ti} + \varepsilon_{bl}C_{bl} \quad (12)$$

$$k_{ti,eff} = (1 - \varepsilon_{bl})k_{ti} + \varepsilon_{bl}k_{bl} \quad (13)$$

where ε_{bl} is the porosity of the tissue where blood flows and T_{ti}^* is the local mean tissue temperature expressed as (Minkowycz et al., 2009)

$$T_{ti}^* = \frac{(1 - \varepsilon_{bl})\rho_{ti}C_{ti}T_{ti} + \varepsilon_{bl}\rho_{bl}C_{bl}k_{bl}}{\rho_{ti,eff}C_{ti,eff}} \quad (14)$$

Since $\varepsilon_{bl} \ll 1$, it follows that $k_{ti,eff}$ is independent of blood flow and equal to the conductivity of the solid tissue (k_{ti}).

Although the Chen-Holmes model represents a significant improvement over Pennes' equation, it is not easy to implement since it requires detailed knowledge of the vascular network and blood perfusion. Furthermore, the model does not explicitly address the effect of closely spaced countercurrent artery-vein pairs (Kreith, 2000).

3.5 Weinbaum, Jiji and Lemons (WJL) bioheat model

The modeling of countercurrent vascular system, which was not explicitly addressed by the Chen-Holmes model, developed separately from that of the continuum models. In 1984, Weinbaum, Jiji and Lemons presented a new vascular bioheat model by considering the countercurrent blood flow. This model was obtained based on a hypothesis that small arteries and veins are parallel and the flow direction is countercurrent, resulting in counterbalanced heating and cooling effects (Fig. 5). It should be noted that this assumption is mainly applicable within the intermediate tissue of the skin (Minkowycz et al., 2009). In an anatomic study performed on rabbit limbs, Weinbaum et al. (1984) identified three vascular layers (deep, intermediate, and cutaneous) in the outer 1cm tissue layer. For the countercurrent structure of the deep tissue layer, they proposed a system of three coupled equations:

$$\rho_{bl}C_{bl}\pi r^2\bar{v}\cdot\frac{dT_{art}}{ds} = -q_{art} \quad (15)$$

$$\rho_{bl}C_{bl}\pi r^2\bar{v}\cdot\frac{dT_v}{ds} = -q_v \quad (16)$$

$$\rho_{ti}C_{ti}\frac{\partial T_{ti}}{\partial t} = \nabla\cdot k_{ti}\nabla T_{ti} + \left\{ ng\rho_{bl}C_{bl}(T_{art} - T_v) - \rho_{bl}C_{bl}n\pi r^2\bar{v}\cdot\frac{d(T_{art} - T_v)}{ds} \right\} + q_m \quad (17)$$

where q_{art} is the heat loss from the artery by conduction through its wall, q_v is the heat gain by conduction per unit length through the vein wall into the vein, T_{art} and T_v are the bulk mean temperatures inside the blood vessel, r is the vessel radius, \bar{v} is the mean velocity in either the artery or vein, n is the number of arteries or veins, and g is the perfusion bleed-off

velocity per unit vessel surface area (s). The first two equations describe the heat transfer of the thermally significant artery and vein, respectively. The third equation refers to the tissue surrounding the artery-vein pair. In Eq. (17), the middle two right-hand-side terms represent the capillary bleed-off energy exchange, and the net heat exchange between the tissue and artery-vein pair, respectively. The capillary bleed-off term is similar to Pennes' perfusion term except the bleed-off mass flow (g) is used. Their analysis showed that the major heat transfer is due to the imperfect countercurrent heat exchange between artery-vein pairs. They quantified the effect of perfusion bleed-off associated with this vascular structure, and showed that Pennes' perfusion formulation is negligible due to the temperature differential (Kreith, 2000).

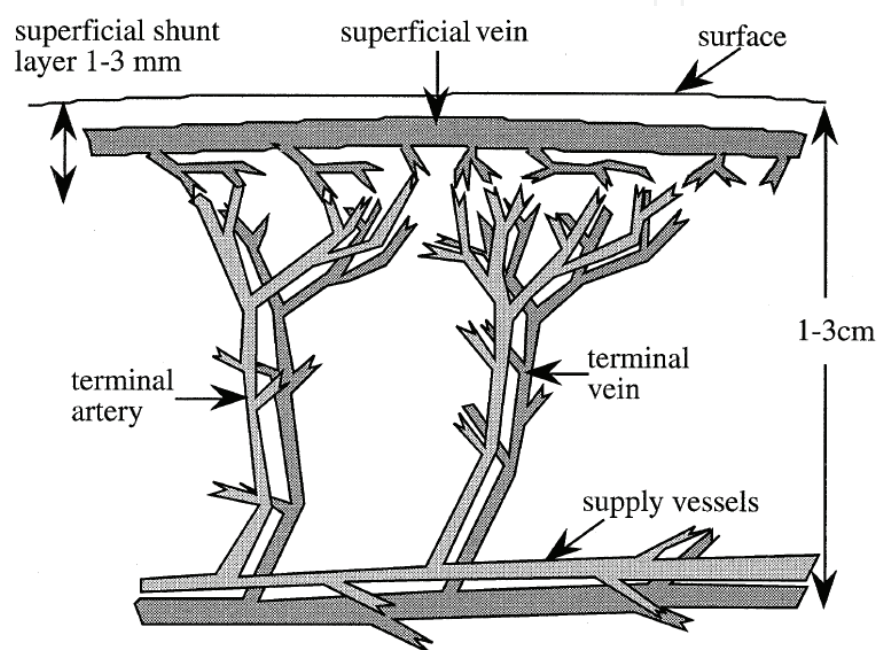


Fig. 5. Schematic of artery and vein pair in peripheral skin layer (Kreith, 2000)

Assumptions of the Weinbaum-Jiji-Lemons model include the following (Kreith, 2000):

1. Neglecting the lymphatic fluid loss, so that the mass flow rate in the artery is equal to that of the vein.
2. Spatially uniform bleed-off perfusion.
3. Heat transfer in the plane normal to the artery-vein pair is greater than that along the vessels (in order to apply the approximation of superposition of a line sink and source in a pure conduction field).
4. A linear relationship for the temperature along the radial direction in the plane normal to the artery and vein.
5. The artery-vein border temperature equals the mean of the artery and vein temperature.
6. The blood exiting the bleed-off capillaries and entering the veins is at the venous blood temperature.

The last assumption has drawn criticism based on studies that indicate the temperature to be closer to tissue. Limitations of this model include the difficulty of implementation, and that the artery and vein diameters must be identical (Kreith, 2000).

3.6 Simplified Weinbaum-Jiji (WJ) model

Since both T_{art} and T_{v} are unknowns in Equation (17), the tissue temperature T_{ti} cannot be determined. Therefore, Weinbaum and Jiji (1985) derived a simplified single equation to study the influence of blood flow on the tissue temperature distribution. In order to eliminate the artery and vein temperatures from their previous formulation (Weinbaum et al., 1984), two major assumptions were used:

1. Tissue temperature T_{ti} is approximated by the average of the local artery and vein temperatures. That is

$$T_{\text{ti}} \approx \frac{T_{\text{art}} + T_{\text{v}}}{2} \quad (18)$$

2. Heat from a paired artery is mostly conducted to the corresponding vein:

$$q_{\text{art}} \approx q_{\text{v}} \approx \sigma_{\Delta} k_{\text{ti}} (T_{\text{art}} - T_{\text{v}}) \quad (19)$$

where σ_{Δ} is a geometrical shape factor and it is associated with the resistance to heat transfer between two parallel vessels embedded in an infinite medium (Jiji, 2009). For the case of vessels at uniform surface temperatures with center to center spacing l , the shape factor is given by (Chato, 1980)

$$\sigma_{\Delta} = \frac{\pi}{\cosh^{-1}(l/2r)} \quad (20)$$

By using the mentioned assumptions and substituting the Eqs. (18) and (19) in Eqs. (15), (16) and (17), Weinbaum and Jiji (1985) proposed a simplified equation for evaluating the tissue temperature distribution:

$$\rho_{\text{ti}} C_{\text{ti}} \frac{\partial T_{\text{ti}}}{\partial t} = \nabla \cdot k_{\text{eff}} \nabla T_{\text{ti}} + q_{\text{m}} \quad (21)$$

where k_{eff} is the effective conductivity, defined as

$$k_{\text{eff}} = k_{\text{ti}} [1 + Pe_i V(\xi)] \quad (22)$$

where ξ is a dimensionless distance and it defines as x/L and L is the tissue layer thickness. Also, $V(\xi)$ is dimensionless vascular geometry function and it can be calculated if the vascular data are available. Furthermore, Pe_i is the inlet Peclet number; which is defined as (Jiji, 2009)

$$Pe_i = \frac{2\rho_{\text{bl}} C_{\text{bl}} r_i v_i}{k_{\text{bl}}} \quad (23)$$

where r_i and v_i are the vessel radius and the blood velocity at the inlet to the tissue layer at $x=0$.

The main limitations of the Weinbaum-Jiji bioheat equation are associated with the importance of the countercurrent heat exchange. It was derived to describe heat transfer in peripheral tissue only, where its fundamental assumptions are most applicable. In tissue area containing a big blood vessel (>200 μm in diameter), the assumption that most of the heat leaving the artery is recaptured by its countercurrent vein could be violated; thus, it is

not an accurate model to predict the temperature field. Furthermore, unlike the Pennes bioheat equation, which requires only the value of local blood perfusion rate, the Weinbaum-Jiji bioheat model requires many detailed anatomical and vascular data such as the vessel number density, size, and artery-vein spacing for each vessel generation, as well as the blood perfusion rate. These anatomic data are normally not available for most blood vessels in the thermally significant range (Kutz, 2009).

4. Bioheat transfer in physiologically controlled tissues

4.1 Thermoregulatory control mechanisms of the human body

Thermoregulation is the ability of an organism to keep its body temperature within certain boundaries, even when the surrounding temperature is very different. The hypothalamus regulates the body temperature by the thermoregulatory mechanisms such as vasomotion, shivering and regulatory sweating. It receives inputs from central and peripheral temperature receptors situated in the 'core' and in the outer 'shell'. Temperature-sensitive receptors in the core are found in the hypothalamus, spinal cord, abdominal viscera and the great veins. They respond to temperatures between 30°C and 42°C. Peripheral receptors are located in the skin and they contain two types of thermoreceptors: warm receptors and cold receptors. The hypothalamic response to a thermal stimulus depends on the integration of both central and peripheral stimuli (Campbell, 2008). The intensity of these stimuli depends on the difference between the temperature of each compartment of the body (core or skin) and its related neutral temperature. In 1988, Doherty and Arens named the mentioned temperature difference as the thermal signals. The thermoregulatory mechanisms of the body are controlled by these thermal signals. The cold and warm signals of human body for skin and core compartments are defined as follows (Doherty & Arens, 1988)

$$WSIG_{cr} = \text{Max}\{0, T_{cr} - T_{cr,n}\} \quad (24)$$

$$CSIG_{cr} = \text{Max}\{0, T_{cr,n} - T_{cr}\} \quad (25)$$

$$WSIG_{sk} = \text{Max}\{0, T_{sk} - T_{sk,n}\} \quad (26)$$

$$CSIG_{sk} = \text{Max}\{0, T_{sk,n} - T_{sk}\} \quad (27)$$

where $CSIG$ and $WSIG$, respectively, represent cold and warm signals of the human body, $T_{sk,n}$ is neutral skin temperature ($\approx 33.7^\circ\text{C}$), and $T_{cr,n}$ is neutral core temperature ($\approx 36.8^\circ\text{C}$). The thermal neutrality state of the human body occurs when the body is able to maintain its thermal equilibrium with the environment with minimal regulatory effort (Yigit, 1999).

The thermoregulatory mechanisms of the human body are related to the aforementioned thermal signals of the body. One of these thermoregulatory mechanisms is vasomotion. Vasomotion of blood vessels (vasoconstriction and vasodilation) is caused by cold/warm thermal conditions and it changes the rate of blood flow (\dot{m}_{bl}) and also the fraction of body mass concentrated in skin compartment (α). These parameters can be calculated as follows (Kaynakli & Kilic, 2005)

$$\alpha = 0.0418 + 0.745 / (3600\dot{m}_{bl} + 0.585) \quad (28)$$

where

$$\dot{m}_{bl} = \frac{6.3 + 200WSIG_{cr}}{3600(1 + 0.5CSIG_{sk})} \quad (29)$$

The other thermoregulatory mechanism of the human body is shivering under cold sensation. Shivering is an increase of heat production during cold exposure due to increased contractile activity of skeletal muscles (Wan & Fan, 2008). Shivering and muscle tension may generate additional metabolic heat. Total metabolic heat production of body includes the metabolic rate due to activity (M_{act}) and the shivering metabolic rate (M_{shiv}). Therefore

$$M = M_{act} + M_{shiv} \quad (30)$$

and

$$M_{shiv} = 19.4CSIG_{sk}CSIG_{cr} \quad (31)$$

Another thermoregulatory mechanism of the body is regulatory sweating. Sweating causes the latent heat loss from the skin. The rate of the sweat production per unit of skin area can be estimated by the following equation (Kaynakli & Kilic, 2005)

$$\dot{m}_{rsw} = 4.7 \times 10^{-5} WSIG_b \exp(WSIG_{sk} / 10.7) \quad (32)$$

where

$$WSIG_b = \text{Max}\{0, T_b - T_{b,n}\} \quad (33)$$

and

$$T_b = \alpha T_{sk} + (1 - \alpha)T_{cr} \quad (34)$$

$$T_{b,n} = \alpha T_{sk,n} + (1 - \alpha)T_{cr,n} \quad (35)$$

where $WSIG_b$ is warm signal of body, T_b is body temperature ($^{\circ}\text{C}$), and $T_{b,n}$ is the neutral temperature of body ($^{\circ}\text{C}$).

The regulatory sweating leads to an increase in the skin wettedness. The total skin wettedness is composed of wettedness due to diffusion through the skin (w_{dif}) and regulatory sweating (w_{rsw}). Therefore

$$w_{skin} = w_{dif} + w_{rsw} \quad (36)$$

where

$$w_{dif} = 0.06(1 - w_{rsw}) \quad (37)$$

$$w_{rsw} = \frac{\dot{m}_{rsw}h_{fg}}{q_{evap,max}} \quad (38)$$

where h_{fg} is the heat of vaporization of water and $q_{evap,max}$ is the maximum evaporative potential and can be estimated by the following equation (Kaynakli & Kilic, 2005)

$$q_{\text{evap,max}} = \frac{P_{\text{sk(s)}} - P_a}{R_{\text{e,t}}} \quad (39)$$

where $P_{\text{sk(s)}}$ is water vapor pressure in the saturated air at the skin temperature (kPa) and $R_{\text{e,t}}$ is the total evaporative resistance between the body and the environment ($\text{m}^2\text{kPa/W}$).

4.2 Simplified thermoregulatory bioheat (STB) model

The human body thermal response may be significantly affected by thermoregulatory mechanisms of the human body such as shivering, regulatory sweating and vasomotion. But, these thermoregulatory mechanisms have not been considered in the well-known Pennes model and also in the other modified bioheat models. In addition, although the body core temperature could be changed depending on personal/environmental conditions, it is commonly assumed as a constant value in Pennes model. Therefore, it seems that the well-known Pennes bioheat model must be modified for using in human thermal response applications. In 2010, Zolfaghari and Maerefat (2010) developed a new simplified thermoregulatory bioheat model (STB model) on the basis of two main objectives: the first is to supplement the thermoregulatory mechanisms to Pennes bioheat model, and the second is to consider the body core temperature as a variant parameter depending on personal/environmental conditions. In order to reach the mentioned objectives, Zolfaghari and Maerefat (2010) developed their bioheat model by combining Pennes' equation and Gagge's two-node model. By using this concept, they presented an energy balance equation for core compartment of the human body as follows

$$(1 - \alpha)\rho_b C_b \frac{dT_{\text{cr}}}{dt} = r_m q_m - \frac{(K_{\text{eff}} + C_{\text{bl}} \dot{m}_{\text{bl}})(T_{\text{cr}} - T_{\text{sk}})}{\ell_b} \quad (40)$$

where ρ_b is specific heat of the body (kg/m^3), C_b is specific heat of body ($\text{J/kg}^\circ\text{C}$), r_m is remaining metabolic coefficient, Q_m is the volumetric metabolic heat generation (W/m^3), K_{eff} is the effective conductance between core and skin compartments, C_{bl} is specific heat of blood ($\text{J/kg}^\circ\text{C}$), and ℓ_b is characteristic length of the body (m) and it is defined as follows

$$\ell_b = \frac{V_b}{A_D} \quad (41)$$

where V_b is the volume of the human body (m^3) and A_D is the nude body surface area (m^2). A_D is described by the well-known DuBois formula (DuBois and DuBois, 1916)

$$A_D = 0.202 m^{0.425} l^{0.725} \quad (42)$$

where m and l are body mass (kg) and height (m). Also, remaining metabolic coefficient (r_m) is defined as follows

$$r_m = 1 - \eta - 0.0014(34 - T_a) - 0.0173(5.87 - P_a) \quad (43)$$

where η is external mechanical efficiency (Fanger, 1970) and

$$\eta = \frac{W}{M} \quad (44)$$

It should be noted that the external mechanical efficiency (η) is insignificant in many human thermal response applications. Also, the respiratory heat losses are negligible compared to the total metabolic rate. Thus, the value of r_m can be approximately estimated as unity.

Discretizing Eq. (40) gives

$$T_{cr}^{new} = T_{cr}^{old} + \frac{\Delta t}{(1-\alpha)\rho_b C_b} \left[r_m q_m - \frac{(K_{eff} + C_{bl} \dot{m}_{bl})(T_{cr}^{old} - T_{sk}^{old})}{\ell_b} \right] \quad (45)$$

Eq. (45) is used as a thermal boundary condition for the human body core in the STB model. By implementing this approach, the core temperature is not treated as a constant value and it varies depending on personal/environmental conditions. Therefore, the main governing equation of the STB model is

$$\rho_{ti} C_{ti} \frac{\partial T_{ti}}{\partial t} = k_{ti} \frac{\partial^2 T_{ti}}{\partial x^2} + \rho_{bl} C_{bl} W_{bl} (T_{art} - T_{ti}) + q_m \quad (46)$$

with time-dependent boundary conditions for skin surface and body core

$$\begin{cases} -k_{ti} \frac{\partial T_{ti}}{\partial x} = h(T_{ti} - T_a) + \sigma \varepsilon ((T_{ti} + 273)^4 - (T_a + 273)^4) \\ \quad + (3.054 + 16.7 h w_{skin})(0.256 T_{ti} - 3.37 - P_a), & \text{at skin surface} \\ T_{cr}^{new} = T_{cr}^{old} + \frac{\Delta t}{(1-\alpha)\rho_b C_b} \left[r_m q_m - \frac{(K_{eff} + C_{bl} \dot{m}_{bl})(T_{cr}^{old} - T_{sk}^{old})}{\ell_b} \right], & \text{at body core} \end{cases} \quad (47)$$

where T_a is the surrounding air temperature, P_a is the water vapor pressure in the air, h is convective heat transfer coefficient, ε is the skin emissivity, and σ is Stefan-Boltzmann constant ($5.67 \times 10^{-8} \text{ W/m}^2 \text{ K}^4$).

It should be noted that some physiological parameters in Eqs. (46) and (47) such as q_m , w_{skin} , α and \dot{m}_{bl} are influenced by thermoregulatory mechanisms. Also, the metabolic heat production is related to the physical activity of the human body and it can be increased by shivering against cold. Hence,

$$q_m = q_{m,act} + q_{m,shiv} \quad (48)$$

and

$$q_{m,shiv} = \frac{19.4 C S I G_{sk} C S I G_{cr}}{\ell_b} \quad (49)$$

Also, skin wettedness (w_{skin}) can be calculated from Eqs. (36) to (39). In addition, α and \dot{m}_{bl} are, respectively, estimated by Eq. (28) and Eq. (29).

Fig. 6 illustrates calculation steps of the STB model (Zolfaghari & Maerefat, 2010). At the beginning, personal and environmental variables are input. Then, the initial temperature distribution in tissue is computed by solving the steady-state bioheat equation under the initial conditions. It should be noted that the steady-state bioheat equation can be obtained by eliminating time dependent derivations in the well-known Pennes bioheat equation.

Afterwards, at each time step, skin and core control signals are calculated and the thermoregulatory parameters are subsequently computed. Then, the temperature distribution in tissue can be obtained by solving the bioheat equation which expressed by Eq. (46) and its related boundary conditions in Eq. (47). Because of the non-linearity of the mentioned equations, they must be solved numerically. Zolafaghari and Maerefat (2010) used the implicit finite difference scheme to find out the temperature distribution of the human body.

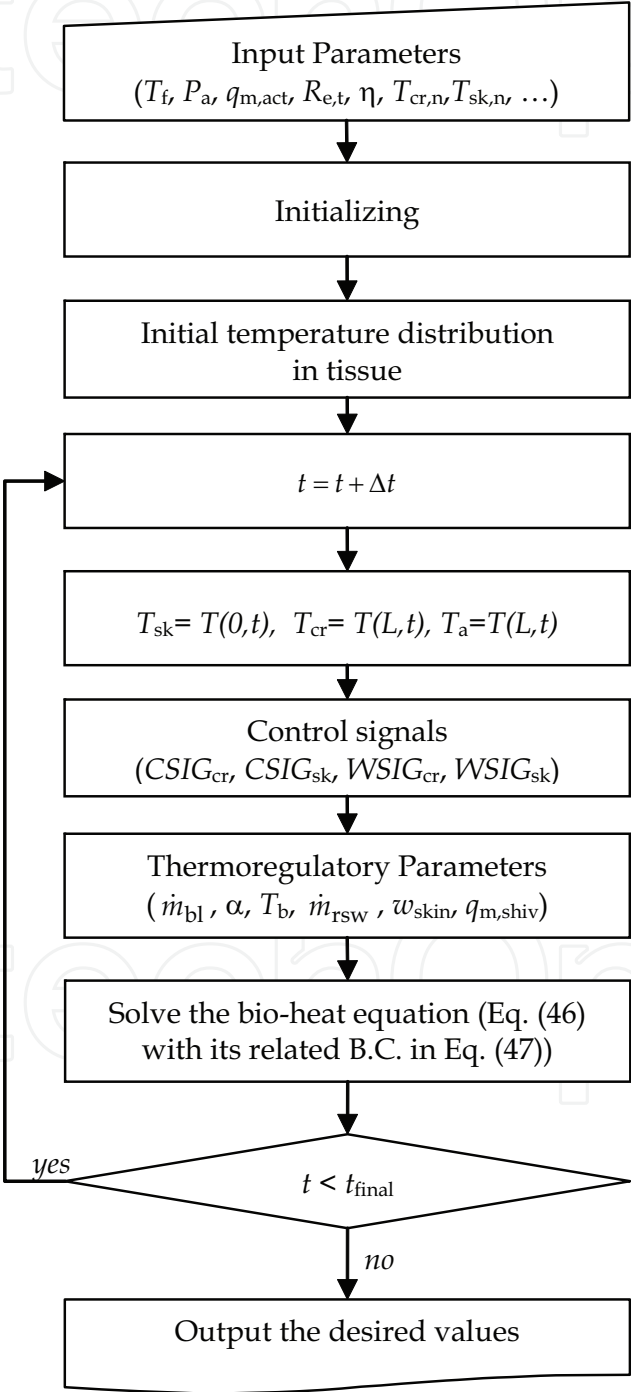


Fig. 6. Flow chart of the STB model calculations

The STB model has been validated against the published experimental and analytical results, where a good agreement has been found. Zolfaghari and Maerefat (2010) showed that the thermal conditions of the human body may be significantly affected by the thermoregulatory mechanisms. Therefore, neglecting the control signals and thermoregulatory mechanisms of the human body can cause a significant error in evaluating the body thermal conditions. Zolfaghari and Maerefat (2010) compared the results of STB model with the results of Pennes bioheat model. This comparison was performed against Stolwijk and Hardy (1966) measured data for a step change in ambient temperature from 30°C/40%RH to 48°C/30%RH for an exposure period of 2 hours followed by 1 hour of environment at 30°C/40%RH. Fig. 7 shows the measured skin temperature data of Stolwijk and Hardy (1966) and the simulation results of Zolfaghari and Maerefat (2010) for STB and Pennes bioheat models. It can be clearly seen that the Pennes bioheat model is not able to accurately estimate the skin temperature under hot environmental conditions. As shown in Fig. 7, the Pennes bioheat model overestimates the value of the skin temperature more than 3.5°C under the mentioned extremely hot conditions. This inaccuracy may be caused by neglecting the thermoregulatory mechanisms such as regulatory sweating and vasomotion in Pennes bioheat model. However, as can be seen in Fig. 7, the results of the STB model are in a good agreement with the experimental results.

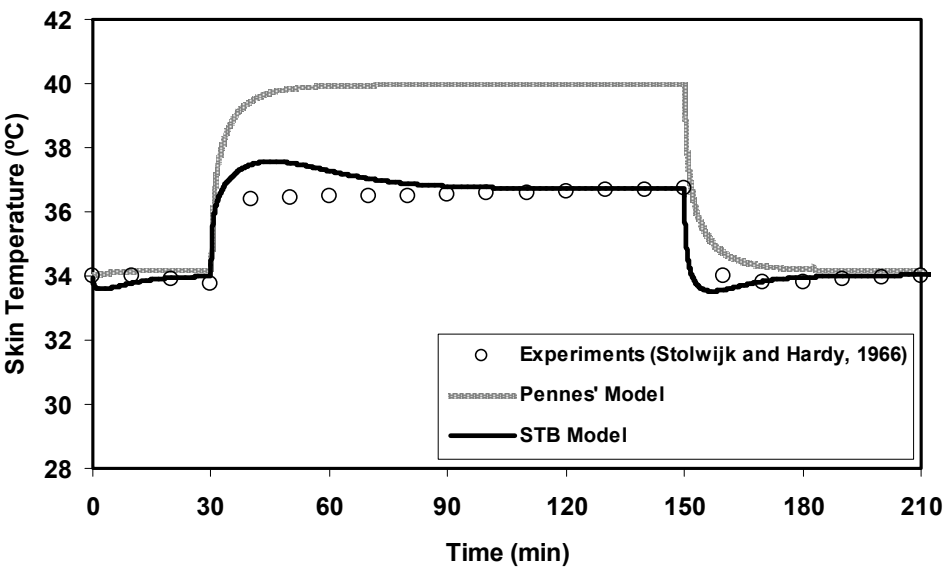


Fig. 7. Comparison of measured (Stolwijk & Hardy, 1966) and simulated skin temperature (Pennes' model and the STB model) during temperature step change

Despite the simplicity of the STB model, it is able to accurately predict the temperature in the cutaneous layer under a wide range of personal/environmental conditions. Also, Zolfaghari and Maerefat (2010) showed that, because of the simplicity and reasonable accuracy of the STB model, it can be widely used in predicting the thermal response of the human body under both transient and steady-state environments. Therefore, the STB model can be utilized for evaluating thermal comfort of the human body in variant personal/environmental conditions. Furthermore, the model validations show that the model results are sufficiently reliable under extremely hot/cold conditions (Zolfaghari & Maerefat, 2010).

5. Conclusion

In this chapter, a brief review of bioheat transfer models (e.g. Pennes' bioheat equation, Wulff Continuum Model, Klinger Continuum Model, Chen-Holmes model, Weinbaum-Jiji-Lemons vascular model and simplified Weinbaum-Jiji vascular Model) has been presented. Also, a new simplified thermoregulatory bioheat (STB) model (Zolfaghari & Maerefat, 2010) has been briefly introduced in the present chapter. The STB model has been developed by combining the well-known Pennes' equation with Gagge's two-node model for evaluating the temperature in the cutaneous layer under a wide range of personal/environmental conditions. This model considers the effects of thermoregulatory mechanisms of the human body by defining the thermal control signals of the body. The STB model has been validated against the published experimental and analytical results, where a good agreement has been found (Zolfaghari & Maerefat, 2010). Therefore, the results of the STB model are sufficiently reliable for estimating the cutaneous temperature under both transient and steady-state thermal conditions.

6. References

- Chato, J.C. (1980). Heat Transfer to Blood Vessels, *ASME Journal of Biomechanical Engineering*, Vol. 102, pp. 110-118, ISSN 0148-0731
- Chen, M.M. & Holmes, K. R. (1980). Microvascular Contributions in Tissue Heat Transfer, *Annals of the New York Academy of Sciences*, Vol. 335, pp. 137-150, ISSN 0077-8923
- Cho, Y.I. (1992). *Bioengineering Heat Transfer*, In: *Advances in Heat Transfer*, J.P. Hartnett & T.F. Irvine, (Ed.), Academic Press, Inc., ISBN 978-0-12-020022-8, San Diego, USA
- Campbell, I. (2008). Body Temperature and its Regulation. *Anaesthesia & Intensive Care Medicine*, Vol. 9, No. 6, pp. 259-263, ISSN 1472-0299
- Datta, A.K. (2002). *Biological and Bioenvironmental Heat and Mass Transfer*, Marcel Dekker, Inc., ISBN 978-0-8247-0775-3, New York, USA
- Doherty, T. & Arens, E.A. (1988). Evaluation of the Physiological Bases of Thermal Comfort Models. *ASHRAE Transaction*, Vol. 94, pp. 1371-1385, ISSN 0001-2505
- DuBois D. & DuBois E.F. (1916) A Formula to Estimate Approximate Surface Area, if Height and Weight are Known. *Archives of Internal Medicine*, Vol. 17, pp. 863-871, ISSN 0003-9926
- Fanger P.O. (1970). *Thermal Comfort Analysis and Applications in Environmental Engineering*, McGraw-Hill, ISBN 0-07-019915-9, New York, USA
- Jiji, L.M. (2009). *Heat Conduction*, Third Edition, Springer, ISBN 978-3-642-01266-2, Berlin, Germany
- Kaynakli O. & Kilic M. (2005). Investigation of indoor thermal comfort under transient conditions. *Building and Environment*, Vol. 40, No. 2, pp. 165-174, ISSN 0360-1323
- Klinger, H.G. (1974). Heat transfer in perfused biological tissue. I. General theory. *Bulletin of Mathematical Biology*, Vol. 36, pp. 403-415, ISSN 1522-9602
- Kreith, F. (2000). *The CRC Handbook of Thermal Engineering*, CRC Press, ISBN 978-0-8493-9581-9, Boca Raton, USA
- Kutz, M. (2009). *Biomedical Engineering and Design Handbook*, Second Edition, McGraw-Hill, ISBN 978-0-07-170472-4, New York, USA
- Lv Y.G. & Liu J. (2007). Effect of transient temperature on thermoreceptor response and thermal sensation. *Building and Environment*, Vol. 42, pp. 656-64, ISSN 0360-1323

- Minkowycz, W.J., Sparrow, E.M. & Abraham, J.P. (2009). *Advances in Numerical Heat Transfer: Volume 3*, CRC Press, ISBN 978-1-4200-9521-0, Boca Raton, USA
- Pennes, H.H. (1948). Analysis of Tissue and Arterial Blood Temperatures in the Resting Forearm, *Journal of Applied Physiology*, Vol. 1, pp. 93-122, ISSN 1522-1601
- Raaymakers, B.W., Kotte, A.N.T.J. & Lagendijk, J.J.W. (2009). Discrete Vasculature (DIVA) Model Simulating the Thermal Impact of Individual Blood Vessels for In Vivo Heat Transfer, In: *Advances in Numerical Heat Transfer: Volume 3*, Minkowycz, W.J., Sparrow, E.M. & Abraham, J.P., pp. 121-148, CRC Press, ISBN 978-1-4200-9521-0, Boca Raton, USA
- Sharma, K.R. (2010). *Transport Phenomena in Biomedical Engineering*, McGraw-Hill, ISBN 978-0-07-166398-4, New York, USA
- Stolwijk J.A.J. & Hardy J.D. (1966). Temperature regulation in man – A theoretical study. *Pflügers Archiv European Journal of Physiology*, Vol. 291, No. 2, pp. 129-62, ISSN 0031-6768
- Vafai, K. (2011). *Porous Media: Applications in Biological Systems and Biotechnology*, CRC Press, ISBN 978-1-4200-6541-1, Boca Raton, USA
- Wan, X. & Fan, J. (2008). A Transient Thermal Model of the Human Body-Clothing-Environment System. *Journal of Thermal Biology*, Vol. 33, pp. 87-97, ISSN 0306-4565
- Weinbaum, S., Jiji, L.M. & Lemons, D.E. (1984). Theory and experiment for the effect of vascular microstructure on surface tissue heat transfer. Part I. Anatomical foundation and model conceptualization. *ASME Journal of Biomechanical Engineering*, Vol. 106, pp. 321-330, ISSN 0148-0731
- Weinbaum, S. & Jiji, L.M. (1985). A new simplified bioheat equation for the effect of blood flow on local average tissue temperature. *ASME Journal of Biomechanical Engineering*, Vol. 107, pp. 131-139, ISSN 0148-0731
- Wulff, W. (1974). The Energy Conservation Equation for Living Tissues. *IEEE Transactions-Biomedical Engineering*, vol. 21, pp. 494-495, ISSN 0018-9294
- Yigit, A. (1999). Combining Thermal Comfort Models. *ASHRAE Transactions*, Vol. 105, pp. 149-158, ISSN 0001-2505
- Zolfaghari, A. & Maerefat, M. (2010). A New Simplified Thermoregulatory Bioheat Model for Evaluating Thermal Response of the Human Body to Transient Environment. *Building and Environment*, Vol. 45, No. 10, pp. 2068-2076, ISSN 0360-1323



Developments in Heat Transfer

Edited by Dr. Marco Aurelio Dos Santos Bernardes

ISBN 978-953-307-569-3

Hard cover, 688 pages

Publisher InTech

Published online 15, September, 2011

Published in print edition September, 2011

This book comprises heat transfer fundamental concepts and modes (specifically conduction, convection and radiation), bioheat, entransy theory development, micro heat transfer, high temperature applications, turbulent shear flows, mass transfer, heat pipes, design optimization, medical therapies, fiber-optics, heat transfer in surfactant solutions, landmine detection, heat exchangers, radiant floor, packed bed thermal storage systems, inverse space marching method, heat transfer in short slot ducts, freezing and drying mechanisms, variable property effects in heat transfer, heat transfer in electronics and process industries, fission-track thermochronology, combustion, heat transfer in liquid metal flows, human comfort in underground mining, heat transfer on electrical discharge machining and mixing convection. The experimental and theoretical investigations, assessment and enhancement techniques illustrated here aspire to be useful for many researchers, scientists, engineers and graduate students.

How to reference

In order to correctly reference this scholarly work, feel free to copy and paste the following:

Alireza Zolfaghari and Mehdi Maerefat (2011). Bioheat Transfer, Developments in Heat Transfer, Dr. Marco Aurelio Dos Santos Bernardes (Ed.), ISBN: 978-953-307-569-3, InTech, Available from:
<http://www.intechopen.com/books/developments-in-heat-transfer/bioheat-transfer>

INTECH
open science | open minds

InTech Europe

University Campus STeP Ri
Slavka Krautzeka 83/A
51000 Rijeka, Croatia
Phone: +385 (51) 770 447
Fax: +385 (51) 686 166
www.intechopen.com

InTech China

Unit 405, Office Block, Hotel Equatorial Shanghai
No.65, Yan An Road (West), Shanghai, 200040, China
中国上海市延安西路65号上海国际贵都大饭店办公楼405单元
Phone: +86-21-62489820
Fax: +86-21-62489821

© 2011 The Author(s). Licensee IntechOpen. This chapter is distributed under the terms of the [Creative Commons Attribution-NonCommercial-ShareAlike-3.0 License](https://creativecommons.org/licenses/by-nc-sa/3.0/), which permits use, distribution and reproduction for non-commercial purposes, provided the original is properly cited and derivative works building on this content are distributed under the same license.

IntechOpen

IntechOpen